An Electrochemical Approach for Designing Thermochemical Bimetallic Nitrate Hydrogenation Catalysts

Kunal M. Lodaya*, Bryan Tang*, Ryan Bisbey, Sophia Weng, Karl S. Westendorff, Wei Lun Toh, Jaeyune Ryu, Yuriy Román-Leshkov, Yogesh Surendranath**

Department of Chemistry, Massachusetts Institute of Technology, Cambridge, Massachusetts 02139, United States

Abstract: Bimetallic alloy catalysts can achieve a diverse range of reactivity inaccessible to pure metals. Classically, catalytic promotion in alloy catalysts has been ascribed to atomic scale cooperativity between the metal constituents. For catalytic reactions that could involve charge transfer to solution, electron flow across a conductive support can be coupled to ionic flow through solution to permit, in principle, bimetallic promotion even in the complete absence of atomic level connectivity between metal constituents. We examine this hypothesis in the context of nitrate hydrogenation, a reaction that is catalyzed almost exclusively by bimetallic catalysts. Using the state-of-the-art PdCu/C catalyst, we show that the overall nitrate hydrogenation reaction proceeds via the electrochemical coupling of the hydrogen oxidation and nitrate reduction half-reactions. Studies of each metal in isolation reveal that Pd exclusively catalyzes the former, while Cu exclusively catalyzes the latter. These findings suggest that nitrate hydrogenation on PdCu alloys proceeds via galvanic coupling of complementary half-reactions on Pd and Cu, obviating the need for atomic scale cooperativity. Based on this mechanistic insight, we design two new nitrate hydrogenation catalysts, RuCu and RuAg, that operate via the same principle with comparable activity to PdCu. This work enables new strategies for the design of bimetallic catalysis for thermochemical transformations, by pairing metals with disparate electrochemical reactivity.

INTRODUCTION

Bimetallic catalysts have an enormous range of reactivity spanning aerobic oxidations, selective hydrogenation of hydrocarbons, small-molecule electrochemical transformations, and cross-coupling reactions.[1–5] Uncovering the origin of enhanced activity and/or selectivity when compared to monometallic counterparts is essential to the rational design of improved catalysts. Classically, the unique reactivity of bimetallic catalysts has been attributed to either "*ligand/strain*" effects or "*ensemble*" effects.[6–10] Ligand/strain effects arise from electronic structure perturbations of one metal on the other, that tune adsorption strengths of intermediates and thereby modulate reactivity.[11] In contrast, ensemble effects refer to the population and distribution of metal atoms proximate to the active site. These effects can alter the adsorption modes of intermediates, introduce spillover of intermediates from one site to another, and encompass catalyst-support interactions.[12] Importantly, all of these classical modes of action in bimetallic catalysis *require intimate, atomic-level contact* between the alloy components.

As a poignant example, the above paradigms have been used to rationalize the reactivity of bimetallic catalysts for nitrate hydrogenation. This reaction, which is of importance in the context of waste-water remediation, has been found to require bimetallic catalysts to proceed at measurable rates.[13] While nitrate can be hydrogenated to a wide diversity of products including NO, NO_2, N_2 and ammonia, the initial hydrogenation from nitrate to nitrite is viewed to be rate limiting.[14,15] For this reaction step in particular, monometallic catalysts all show greatly reduced or no activity. The two metals paired for thermochemical nitrate hydrogenation are typically a noble metal such as Pd or Pt alongside a "promoter" metal, such as Cu, In, or Sn, with PdCu being the most well-studied and best-performing pairing.[16–23] Various proposals have been offered to explain the enhanced activity compared to monometallic systems and the respective role of each metal. The prevailing hypotheses include hydrogen spillover from Pd sites to Cu sites, or Langmuir-Hinshelwood bimolecular recombination at mixed PdCu active sites.[15,24,25] Both mechanisms align with the classical picture of bimetallic catalysis, requiring atomic-level contact between the two metals.

In recent years, there has been a growing appreciation that liquid-phase thermochemical catalysis can proceed via the electrochemical coupling of countervailing half-reactions mediated by the exchange of band-electrons.[26–28] This band-mediated mechanism for liquid-phase thermochemical catalysis was shown to be operative across a range of aerobic oxidations in monometallic catalyst systems[29] and has been applied in the context of H_2O_2 synthesis on a variety of Pt- and Pd-based catalysts.[30] This mechanism has also been shown to be operative for aerobic hydroquinone oxidation at molecular active sites embedded within metallic solids.[31] Recently, a band-mediated catalytic mechanism was also suggested for an alloy system conducting aerobic oxidation at AuPd catalyst active sites.[32] Here, simple mixtures of Au/C and Pd/C display activity enhancements for alcohol oxidation, though the electrochemical

mechanism underpinning this reactivity remains ill-defined. Given that many of the constituent metals employed for thermochemical nitrate hydrogenation also display activity for electrochemical nitrate reduction,[33–37] we postulated that band mediated mechanisms may be operative for this reaction class as well, and that electrochemical analysis of this reaction could shed light on the origin of bimetallic promotion.

Despite the growing appreciation of the role of electrochemical pathways in thermochemical catalysis, to the best of our knowledge, there remains little insight into how electrochemical reactions partition across bimetallic catalysts. For example, in one limiting extreme, each individual component of the bimetallic system is capable of carrying out both half reactions. In this limit, despite an electrochemical coupling mechanism, the aggregate activity of the alloy is expected to be an ad-mixture of the activities of each individual component. However, in the other limiting extreme, wherein each alloy component is only able to carry out one of the half reactions, electrical contact, but not atomic level contact, between alloy components is the *sole* prerequisite for carrying out the overall reaction. Consequently, distinguishing between these two limiting cases has important implications for the design of high-performance alloy catalysts.

Herein, we show that nitrate hydrogenation to nitrite on PdCu/C proceeds via the latter extreme. Using electrochemical tools, we show that Pd carries out electrochemical hydrogen oxidation to protons and electrons and has no activity for nitrate reduction. In contrast, we find that Cu is active for nitrate reduction with no activity for hydrogen oxidation. This complete separation in the functional role of each alloy component offers a new paradigm for the design of bimetallic catalysts for the net thermochemical reaction by pairing pure metals with electrocatalytic activity for each complementary half-reaction. Employing this strategy, we identify RuCu/C and RuAg/C as new alloys for nitrate hydrogenation catalysis with equal or improved performance relative to state-of-the-art PdCu/C. These results highlight how electrochemical analysis of thermal reactions provides new opportunities for catalyst discovery.

RESULTS AND DISCUSSION

PdCu/C performs hydrogen oxidation and nitrate reduction over a common range of potentials

To examine whether a band-mediated electrocatalytic mechanism is operative for thermochemical nitrate hydrogenation to nitrite, we deployed a similar experimental framework to that used in our previous studies of aerobic oxidation catalysts.[29,31] Briefly, we collect voltammetric data for the putative electrochemical half-reactions that comprise the net thermochemical transformation. By applying a current matching condition to the electrochemical data for each half-reaction in isolation, we extract a predicted mixed-potential and reaction rate for the net thermochemical reaction. Comparing these values to those measured under hydrogenation conditions provides a quantitative measure of whether a band-mediated electrocatalytic mechanism is operative.

Electrochemical measurements and thermochemical reaction data were collected under two electrolyte and pH conditions. For the majority of experiments, 0.1 M KNO_3 + 0.2 M KOH (pH 13) was used to enable faster reaction rates as well as a simplified product distribution. Experiments yielding key findings were then expanded to 0.1 M KNO_3 + 0.5 M phosphate buffer (pH 6.7) to more closely approximate typical experimental conditions probed in the literature.[16] To draw direct comparisons between electrochemical and thermochemical measurements, we fabricated electrodes suitable for both modes of study. Critically, these electrodes required both high catalyst loading and efficient gas transport of H_2 to achieve high thermochemical reaction rates of hydrogenation with minimal effects from H_2 diffusion limitations. Thus, we employed gas-diffusion electrodes (GDEs) with drop-cast catalysts for all measurements (catalyst synthesis, characterization, electrode fabrication and experimental details in **Supplementary Information**). PdCu/C at a 10:90 ratio of Pd:Cu was chosen to begin this investigation because of the extensive body of research on nitrate hydrogenation with this particularly alloy.[16,19,20]

We began by measuring steady-state polarization behavior via linear-sweep voltammetry (LSV) at 2 mV s^{-1} on a PdCu/C GDE. These measurements were performed under two conditions: 1) 1 atm H_2, with no KNO_3 and 2) 0.1 M KNO_3 under 1 atm Ar. In the presence of H_2 and the absence of nitrate, we observe the onset of anodic current beginning at 0 V vs RHE, rising to 5 mA cm^{-2} at ca. 0.3 V vs RHE (**Figure 1a, red**). In contrast, in the presence of nitrate and absence of H_2, we observe the onset of cathodic current at ca. 0.35 V vs RHE, with 20 mA cm^{-2} observed at ca. 0.1 V vs RHE (**Figure 1a, blue**). These data suggest that PdCu/C is capable of catalyzing two distinct half-reactions depending on the reaction conditions: the hydrogen oxidation reaction (HOR) and the nitrate reduction

reaction (NO_3RR). Importantly, the potential range for NO_3RR matches that of HOR, with equal and opposite currents at ca. 0.28 V vs RHE (**Figure 1a**, vertical dotted line). Subjecting the same PdCu/C GDE to thermochemical catalysis conditions − with both NO_3^- and H_2 present – we observe that the open circuit potential (OCP) of the catalyst rapidly reaches a steady-state value of 0.27 V vs RHE (**Figure 1b**, **Supplementary Figure 20**). The same analysis was conducted with a different formulation of PdCu at 50:50 ratio, yielding a predicted OCP of 0.17 V and a measured value of 0.18 V (**Supplementary Figure 21**). Likewise, the same experiment conducted under neutral pH conditions returns a predicted OCP of 0.03 V and a measured value of 0.03 V (**Supplementary Figure 23**). The close agreement between the measured OCP values and those predicted from the independent electrochemical data on each half reaction supports a mechanistic picture for nitrate hydrogenation that involves the electrochemical coupling of independent HOR and NO_3RR half-reactions.

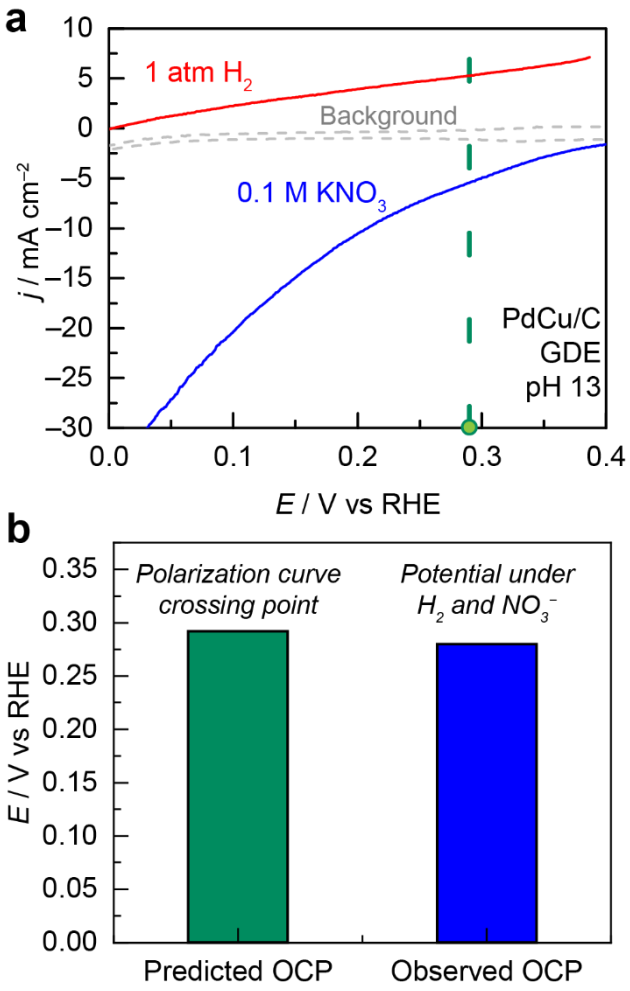

Fig. 1 | (a) Polarization curves collected via LSV at 2 mV/s scan rate of a PdCu/C GDE in 0.2 M KOH. Grey trace (background) was collected under 1 atm Ar. Blue trace (NO_3RR) was collected under 1 atm Ar + 0.1 M KNO_3. Red trace (HOR) was collected under 1 atm H_2. Light blue dashed line indicates the potential at which the currents for the blue and red traces are equal and opposite. All potentials are referenced to RHE. All current densities are normalized with respect to the geometric surface area of the electrode. **(b)** OCP value under thermochemical reaction conditions (1 atm H_2 + 0.1 M KNO_3), predicted from the polarization curves (green), and measured (blue).

Although this OCP data is highly suggestive of an electrochemical mechanism being operative during nitrate hydrogenation catalysis, it does not exclude an electrochemical mechanism proceeding in parallel with a classical thermochemical sequence for nitrate conversion. In this context, an electrochemical mechanism involves electron transfer between the catalyst and each substrate (H_2 and NO_3^-), while a thermochemical mechanism involves

bimolecular recombination of surface-bound NO_3 and surface H species. While the foregoing OCP measurements confirm that HOR and NO_3RR are operative during hydrogenation, a concurrent thermochemical mechanism would be invisible to this probe. To quantify the contribution of the electrochemical mechanism to the overall hydrogenation rate, we compared the rate of nitrate conversion predicted by the polarization data to the observed rate measured during hydrogenation catalysis.

Performing extended reaction measurements at the OCP, bulk conversion of nitrate to nitrite was achieved via reaction with H_2 using a PdCu/C catalyst immobilized on the same electrodes prepared for electrocatalytic measurements. UV-Vis spectroscopy provides a convenient and reproducible route to quantifying mixed solutions of nitrate and nitrite (**Figure 2a**); the method for peak identification and deconvolution of nitrate and nitrite peaks which allowed us to accurately quantify both species simultaneously is discussed in detail in the **Supplementary Methods**. Using this method, nitrate consumption and nitrite generation are both measured during thermochemical catalysis at the PdCu/C GDE, with nitrite identified as the sole product under these conditions (**Figure 2b**). This observation agrees with previous reports of the deactivation of subsequent nitrite hydrogenation under alkaline conditions for this alloy.[38,39] Based on this product distribution, we can now describe the two coupled half-reactions occurring at the OCP at PdCu: the two-electron reduction of NO_3^- to NO_2^-, and the two-electron oxidation of H_2 to H^+.

$$NO_3^- + 2e^- + 2H^+ \rightarrow NO_2^- + H_2O \quad (1)$$

$$H_2 \rightarrow 2e^- + 2H^+ \quad (2)$$

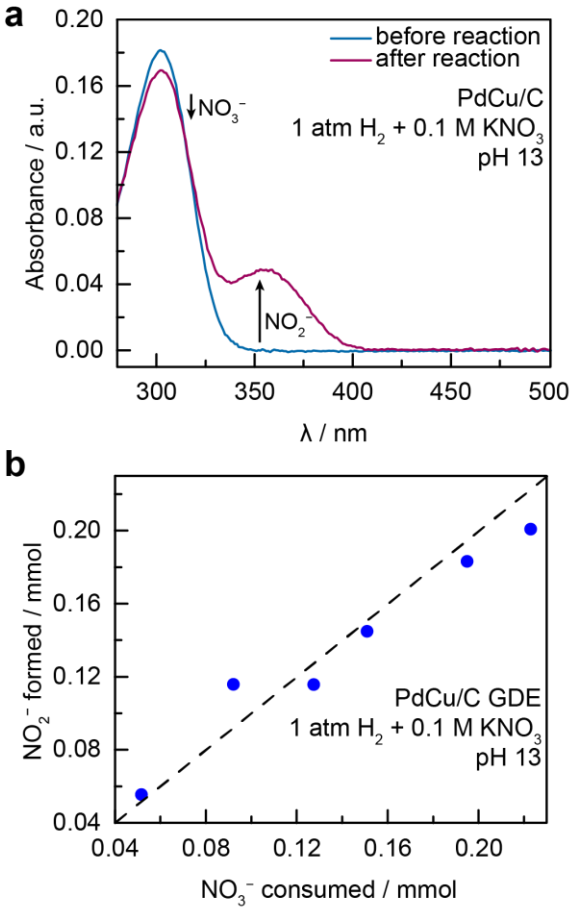

Fig. 2 | (a) Representative UV-Vis spectra of a filtered reaction solution of 0.1 M KNO_3 in 0.2 M KOH. Spectra were collected before and after ~1 hour of nitrate hydrogenation with PdCu/C. Nitrite is observed ca. 370 nm, and nitrate is observed ca. 300 nm. **(b)** Measurements of nitrate consumption and nitrite formation at various timepoints during hydrogenation at PdCu/C GDE. Dashed line included as a visual aid to denote unity.

Armed with this electron stoichiometry, we can predict the thermal hydrogenation rate directly from the electrochemical polarization data, via the current passed by both half-reactions at the crossover potential (**Figure 1a**). After then running the hydrogenation, a thermal rate can be obtained via the disappearance of nitrate or the appearance of nitrite. Converting this rate to an effective current using the electron stoichiometry, the rate of nitrate conversion can be directly compared to the value predicted by the electrochemical data. If the major mechanism were invisible to our electrochemical probes and was thermochemical in nature, we would observe large differences in the measured and predicted reaction rates. On the other hand, if an electrochemical mechanism plays a significant role in the total conversion, we would expect agreement between these rates. The polarization studies predict a current of 5.3 mA, which from the above electron stoichiometry equals 0.027 μmol NO_3^- s^{-1}. A striking agreement is observed with the observed hydrogenation rate of 0.026±0.002 μmol NO_3^- s^{-1}, which can be converted to an effective current of 5.0±0.4 mA. (**Figure 3**). The same current matching is reproduced at a PdCu catalyst with a 50:50 ratio of Pd:Cu (**Supplementary Figure 22**). These data indicate that nitrate hydrogenation at PdCu/C proceeds primarily via an electrochemical mechanism.

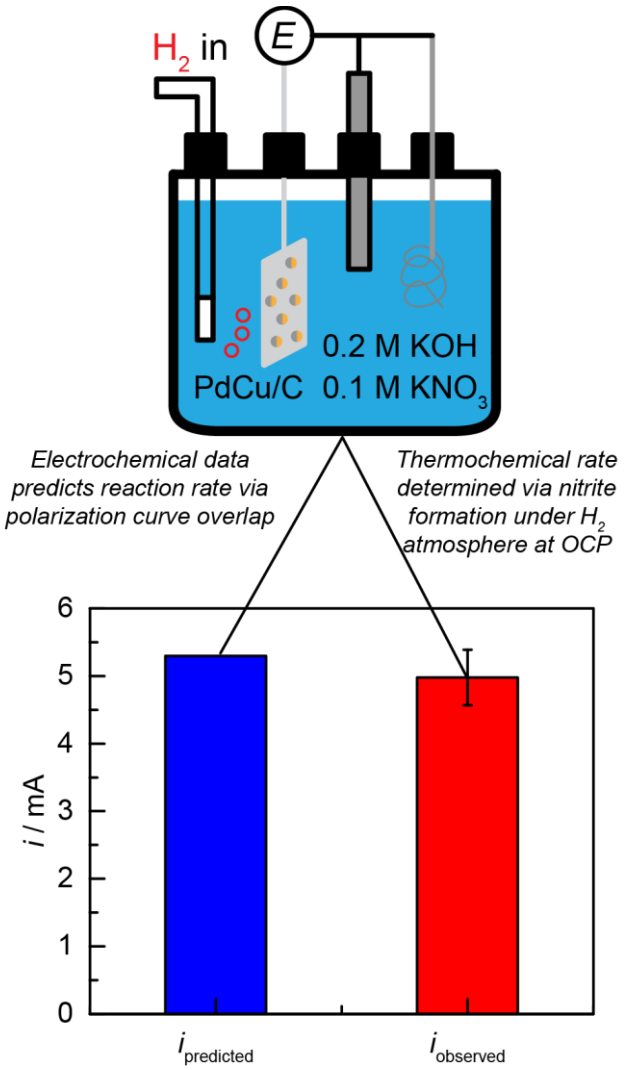

Fig. 3 | Comparison of predicted and observed reaction rates (reported in terms of current) for nitrate hydrogenation to nitrite at PdCu/C. Predicted reaction rate derived from electrochemical data described in Figure 1. Observed reaction rate determined during hydrogenation at a PdCu/C GDE at open circuit in 0.2 M KOH + 0.1 M KNO_3 under 1 atm H_2.

Pd and Cu execute orthogonal electrochemical reactivity to hydrogenate nitrate

Critically, the data presented thus far on PdCu alloy catalysts do not contain any mechanistic information on the individual roles of Pd and Cu in the overall reaction. Initial insight into the role of each metal was obtained by comparing the OCP across a series of PdCu alloy catalysts of varying metal ratios. PdCu alloys were prepared using modified literature methods at different Pd/Cu ratios and dropcast onto carbon electrodes (See **Supplementary Information Section 3** for detailed characterization of each PdCu alloy). These alloy-decorated electrodes were exposed to thermochemical hydrogenation conditions while monitoring their potential at open circuit. Whereas the 10:90 alloy displays an OCP of 0.27 V, this value decreases to 0.18 V for the 50:50 alloy, and decreases further to 0.12 for the 90:10 alloy (**Figure 4**). This monotonic shift of 150 mV with increasing Pd content evinces a distinct electrochemical role for each of these metals. If both metals were competent for both half reactions and displayed similar mixed potentials, we would expect no substantial shift in the overall potential of the alloy as a function of ratio of metal components. At the opposite extreme, if each metal were only competent for one half reaction, then the OCP of the alloy should shift monotonically with alloy composition. A negative OCP shift indicates either that the oxidative half reaction is accelerating or that the reductive half reaction is decelerating, or both (see **Supplementary Figure 27** for a schematic diagram). We observe that the OCP shifts negatively as the Pd content increases, indicating that Pd is preferentially competent for the hydrogen oxidation half reaction relative to Cu and vice versa.

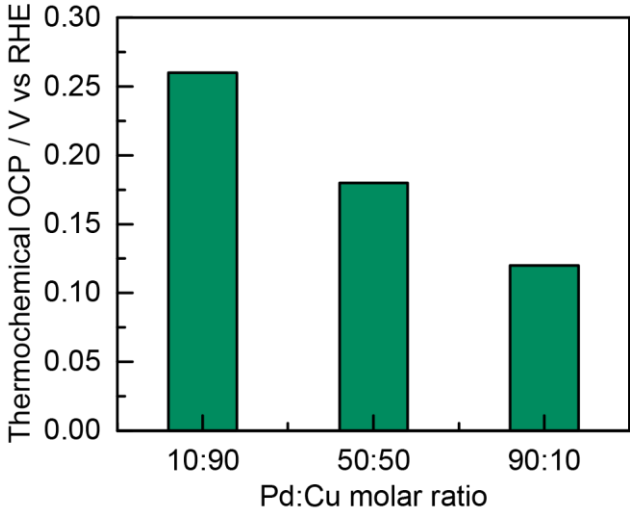

Fig. 4 | Open-circuit potential measurements for alloys of Pd and Cu at various molar ratios Pd:Cu. Potential was measured following equilibration to steady-state in 0.2 M KOH + 0.1 M KNO_3 with 1 atm H_2 (thermal hydrogenation conditions). Transient data is provided in **Supplementary Figure 20**.

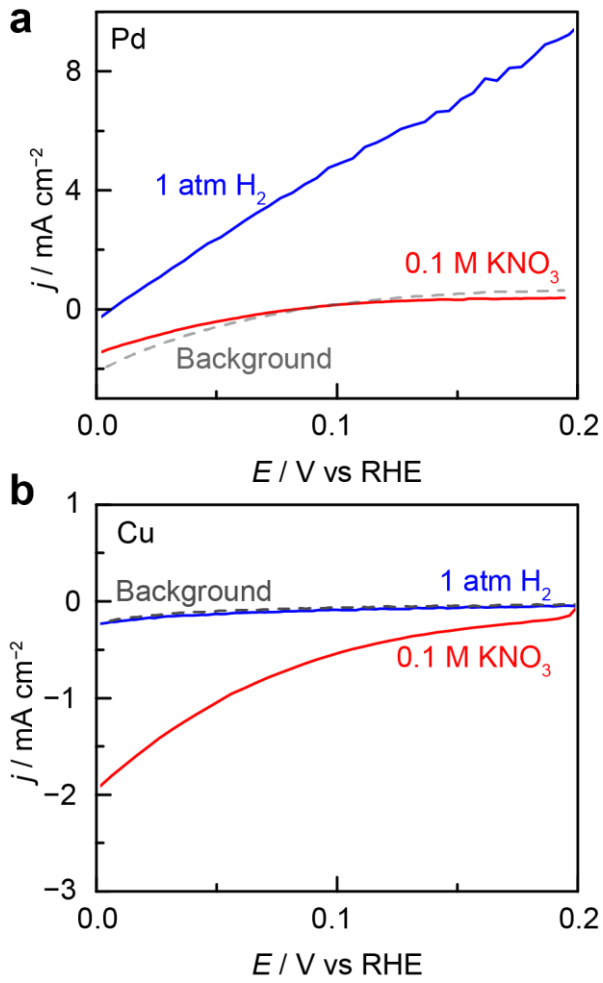

Fig. 5 | Polarization curves recorded via LSV at 2 mv s^{-1} in 0.5 M phosphate buffer (pH = 6.7) for both Pd/C and Cu/C electrodes. Background collected under 1 atm Ar. 0.1 M KNO_3 trace collected under 1 atm Ar. Electrodes used as received, at nominal loadings of 0.5 mg cm^{-2}, 60 wt% for Pd/C, and 0.4 mg cm^{-2}, 40 wt% for Cu/C.

Based on the preceding observation that each metal is not equally competent for each half reaction, we investigated the most extreme case in which one alloy component is excluded entirely. As is well documented in the literature, almost all pure metals are completely inactive for nitrate hydrogenation.[13,20] However, based on the preceding data, we posited that each metal could be competent for one electrochemical half reaction. Indeed, electrochemical polarization data of the two metals prepared as individual catalysts unambiguously demonstrates the orthogonal reactivity of Pd and Cu. Pd/C and Cu/C electrodes were examined using the same electrochemical polarization protocol as employed for PdCu/C (**Figure 5**). Under H_2, Pd displays onset of anodic catalytic current at 0 V vs RHE corresponding to HOR, rising to 4 mA cm^{-2} at 0.1 V vs RHE (**Figure 5a, blue)**. However, in nitrate solution, Pd displays no current enhancement relative to the Ar background (**Figure 5a, red vs gray)**. The same experiments on Cu reveal the opposite reactivity profile, with catalytic current observed in nitrate solution at an onset potential of 0.2 V, rising to 2 mA cm^{-2} cathodic current at 0 V vs RHE (**Figure 5b, red**), but no catalytic current in the presence of H_2 alone (**Figure 5b, blue vs gray**). These data, taken together with the studies above, suggest that in the PdCu alloy, the role of Pd is to oxidize H_2, and the role of Cu is to reduce NO_3^-. It is still possible, as has been suggested previously, that bimetallic active sites also execute this reaction.[15] For example, reactive H atoms formed via H_2 dissociative adsorption at Pd may react with proximate NO_3^- activated at Cu to achieve the same transformation. However, these results strongly suggest that there is no *necessity* for these atomic-level interactions and that their presence confers no substantial catalytic promotion.

Based on this reaction orthogonality, we predict that nitrate hydrogenation can be catalyzed by Pd and Cu at entirely separated interfaces, so long as an electronic conduction path is maintained between the two metals. Indeed, even for Pd/C and Cu/C catalysts that are macroscopically separated by an ion-exchange membrane, shorting the two catalysts is sufficient to drive net nitrate hydrogenation (**Supplementary Figure 24**). Incorporating an ammeter, we observe current flow of ca. 0.5 mA during overall nitrate hydrogenation. By integrating the current flowing in this galvanic cell, we find that the charge passed matches the expected 2-electron stoichiometry of nitrate reduction to nitrite (**Supplementary Figure 25**). Taken together with our findings on PdCu/C, these results suggest that the predominant mechanism by which nitrate is hydrogenated to nitrite is via galvanic coupling between Pd-catalyzed HOR and Cu-catalyzed NO_3RR.

The foregoing data suggest a revision of the prevailing mechanistic picture of nitrate hydrogenation on Pd/Cu bimetallic catalysts. Previously invoked ensemble effects such as spillover of H from Pd to Cu or bimetallic recombination of adsorbed H and surface-bound NO_3 at adjacent PdCu active sites are not necessary for nitrate hydrogenation. Instead, all that is necessary is an electrical pathway for current flow from Pd to Cu and ionic flow of H^+ in solution, rather than any atomic-level interaction between the two constituents. We stress that atomic-level interactions may confer a benefit in certain cases for nitrate hydrogenation catalysts; in particular, we are intrigued by the possibility that well-ordered intermetallic PdCu catalysts with greater proportions of bimetallic active sites may operate via a distinct mechanism. Nevertheless, on typical bimetallic catalysts with lesser degrees of order studied here and in the majority of literature reports, these results strongly support the notion that classical interpretations of bimetallic catalyst activity are insufficient to describe systems involving electrochemical coupling. In these systems, even spatially-separated, but electrically connected combinations of metals can execute reactivity inaccessible to either metal on its own.

Galvanic coupling mechanism guides new catalyst discovery

The observation of a galvanic coupling mechanism for nitrate hydrogenation suggests a rational strategy for developing new alloy catalysts. In particular, the foregoing data would suggest that pairing any electrocatalyst competent for HOR with any electrocatalyst competent for NO_3RR should furnish an effective alloy catalyst for overall nitrate hydrogenation.

To identify candidate metals for integration into alloys for nitrate hydrogenation catalyst, we leveraged the extensive electrochemical studies of HOR and NO_3RR across metals. Ag was recently shown to be an effective NO_3RR catalyst[33] and Pt and Ru are known to display HOR activity.[40] Notably, monometallic Ru has also been shown to have limited activity for nitrate hydrogenation, though much reduced compared to bimetallic catalysts.[41] In our own hands, we observe NO_3RR activity on Ag but no HOR activity, while Pt and Ru display HOR activity and only nominal NO_3RR activity in accordance with previously reported literature (**Supplementary Figure 26**). As a result, we hypothesized that any pairing of Pt or Ru with Cu or Ag would result in a competent nitrate hydrogenation catalyst. PtCu/C and PtAg/C have been previously reported as nitrate hydrogenation catalysts, and we synthesized and measured the activity of the latter (**Figure 6**).[18] The hydrogenation activity of PtAg/C along with the respective electrochemical reactivity of Pt and Ag suggests that this bimetallic catalyst proceeds via the same mechanism we describe for PdCu/C. In contrast to the Pt- and Pd-based bimetallic catalysts, RuCu/C and RuAg/C have not been previously reported for nitrate hydrogenation to the best of our knowledge; these alloys have been previously employed in the hydrolysis of ammonia borane and the hydrogenation of citral.[42,43] Here, we find that both of these alloys have comparable or greater activity for nitrate hydrogenation when compared to the state-of-the-art PdCu/C, evaluated at equivalent metal loadings (25 wt% of 50:50 Pd/Cu vs 25 wt% of 50:50 metal ratio for the other three catalysts) (**Figure 6**). We also observe a shift in product selectivity for these two catalysts, with RuCu/C and RuAg/C producing predominantly ammonia during alkaline nitrate hydrogenation (**Supplementary Table 2)**. Previous studies of nitrate and nitrite hydrogenation typically ascribe higher-order reduction (past nitrite) to Pt or Pd rather than Cu. Thus, in this case, we posit that Ru drives the downstream selectivity to ammonia, given that Cu and Ag do not further reduce nitrite when coupled with Pd and Pt, respectively. In line with this hypothesis, we find that Ru by itself capably catalyzes alkaline nitrite reduction (**Supplementary Table 3)**. These findings highlight the use of electrochemical trends to drive the development of thermochemical nitrate hydrogenation catalysts.

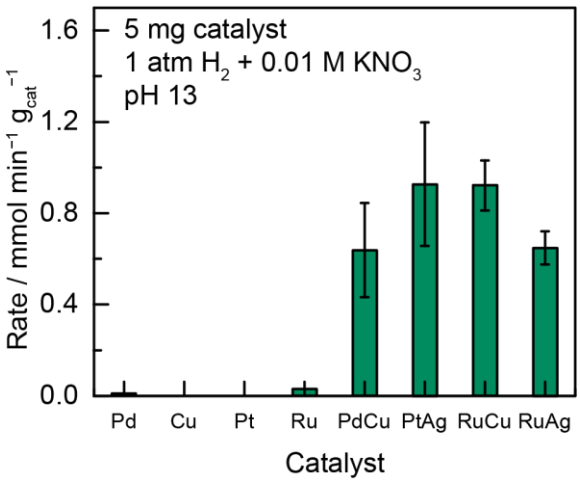

Fig. 6 | Thermochemical reaction rate data for a variety of monometallic and bimetallic nitrate hydrogenation catalysts. Error bars represent standard deviation of at least three rate measurements.

The foregoing studies establish a blueprint for alloy catalyst design that consists of (a) breaking down a net thermochemical reaction into its constituent electrochemical half-reactions (b) identifying viable pure metal catalysts for each half reaction, and (c) combining these pure metals with an electrically conducting support to form new alloy catalysts for the overall reaction. This strategy for discovering new thermochemical bimetallic hydrogenation catalysts is generalizable, and is limited only by the scope of the electrochemical activity of the metals in the periodic table. As opposed to classical trial-and-error approaches for screening the large matrix of metal alloy combinations and composition ratios for net thermochemical activity, electrochemical analysis of the far smaller matrix of pure metals for each putative half reaction provides the necessary information for identifying active alloy catalysts for the overall reaction. Indeed, in this case, the extensive existing electrochemical literature on nitrate reduction and hydrogen oxidation reactions was sufficient to identify new high activity alloys for nitrate hydrogenation. We note that thermochemical nitrate hydrogenation has now been studied for three decades, with PdCu arguably remaining the state-of-the-art catalyst for that entire time.[13,16,44,45] Our electrochemical approach rapidly identified two new alloys that, to the best of our knowledge, have not been previously reported for this reaction. We stress that synthesizing these catalysts was not part of a high-throughput materials discovery effort. Instead, we employed the mechanistic insights described herein combined with known reactivity profiles in electrocatalysis to discover new thermochemical hydrogenation catalysts. Such an approach may prove even more powerful when applied in oxidative thermal catalysis, where a wider array of metals (including non-noble metals) are active for the oxygen reduction half-reaction. This study highlights how electrochemical insights can be used to accelerate the discovery of thermochemical alloy catalysts.

CONCLUSIONS

In this study, we employ an electrochemical toolkit to examine the mechanism of thermochemical nitrate hydrogenation, and create a framework for predictive bimetallic catalysis that leads to the discovery of two alloy catalysts competent for this reaction. Specifically, electrochemical studies suggest that PdCu/C carries out nitrate hydrogenation via band-mediated coupling of HOR occurring exclusively on Pd and NO_3RR occurring exclusively on Cu. These findings challenge the notion that intimate atomic-level contact between metals is critical to alloy reactivity and suggest that galvanic coupling may be a key mechanistic contributor. Employing these insights and leveraging known electrochemical reactivity trends, we rationally designed two new alloy catalysts, both of which display comparable or enhanced activity relative to the state-of-the-art PdCu/C. Historically, the search for new bimetallic catalysts for a given reaction involved the exploration of a massive design space of potential choices in metal constitution, metal-metal ratio, and support.[46] Classical approaches to design within these constraints consist of selecting the primary and dopant metals, followed by high-throughput screening to optimize parameters.[46,47] Because this catalyst test space can easily exceed hundreds or thousands of possible combinations, computational methods such as response surface methodology and machine learning are often employed to pare down to the most likely candidate catalysts.[48–50] Within this context, our work provides a complementary workflow for bimetallic catalyst

design: (1) breaking down thermal reactions into electrochemical half-reactions (2) identifying catalyst components with orthogonal, complementary electrochemical activity (3) pairing these catalyst components to form an active multi-component catalyst. Thus, our findings advance new electrochemical mechanisms for the catalytic reactivity of alloys that enable new strategies for catalyst design and optimization for thermochemical redox transformations.

Data availability

The data that support the findings of this study are included in the published article (and its Supplementary Information) or available from the corresponding author on reasonable request.

Corresponding Author

Correspondence to Yogesh Surendranath: yogi@mit.edu

Acknowledgements

We thank T. Wesley, W. Howland, M. Huelsey, A. Chu, A. Borisov, H-X. Wang, D. Harraz, and the Surendranath Lab for helpful discussions and manuscript feedback. This work was primarily supported by the Air Force Office of Scientific Research (AFOSR) under award number FA9550-20-1-0291. K.M.L., S.W. and K.S.W. acknowledge support from the National Science Foundation Graduate Fellowship.

Author Contributions

K.M.L, B.Y.T, R.B., J.R. and Y.S. conceived the research and developed experiments. K.M.L and B.Y.T conducted all electrochemical and thermochemical experiments. K.M.L., B.Y.T., S.W. and K.S.W. conducted catalyst characterization measurements. W.L.T 3-D printed prototype cell designs for experiments. K.M.L. and Y.S. wrote the manuscript with input from all authors.

Competing Interests

The authors declare no competing interests.

References

1. Park, K.-W. *et al.* Chemical and Electronic Effects of Ni in Pt/Ni and Pt/Ru/Ni Alloy Nanoparticles in Methanol Electrooxidation. *J. Phys. Chem. B* **106**, 1869–1877 (2002).
2. Qin, L. *et al.* Cooperative catalytic performance of bimetallic Ni-Au nanocatalyst for highly efficient hydrogenation of nitroaromatics and corresponding mechanism insight. *Appl. Catal. B Environ.* **259**, 118035 (2019).
3. Muneeb, O. *et al.* Electrochemical Oxidation of Polyalcohols in Alkaline Media on Palladium Catalysts Promoted by the Addition of Copper. *Electrochimica Acta* **218**, 133–139 (2016).
4. Wang, H. *et al.* Platinum-Modulated Cobalt Nanocatalysts for Low-Temperature Aqueous-Phase Fischer–Tropsch Synthesis. *J. Am. Chem. Soc.* **135**, 4149–4158 (2013).
5. Lortie, M., Isaifan, R., Liu, Y. & Mommers, S. Synthesis of CuNi/C and CuNi/ γ -Alcatalysts for the reverse water gas shift reaction. *Int. J. Chem. Eng.* **2015**, (2015).
6. Li, H., Shin, K. & Henkelman, G. Effects of ensembles, ligand, and strain on adsorbate binding to alloy surfaces. *J. Chem. Phys.* **149**, 174705 (2018).
7. Li, H. *et al.* Oxygen Reduction Reaction on Classically Immiscible Bimetallics: A Case Study of RhAu. *J. Phys. Chem. C* **122**, 2712–2716 (2018).
8. Takehiro, N., Liu, P., Bergbreiter, A., Nørskov, J. K. & Behm, R. J. Hydrogen adsorption on bimetallic PdAu(111) surface alloys: minimum adsorption ensemble, ligand and ensemble effects, and ensemble confinement. *Phys. Chem. Chem. Phys.* **16**, 23930–23943 (2014).
9. Mavrikakis, M., Hammer, B. & Nørskov, J. K. Effect of Strain on the Reactivity of Metal Surfaces. *Phys. Rev. Lett.* **81**, 2819–2822 (1998).
10. Zhang, L. & Henkelman, G. Tuning the Oxygen Reduction Activity of Pd Shell Nanoparticles with Random Alloy Cores. *J. Phys. Chem. C* **116**, 20860–20865 (2012).
11. García-Muelas, R. & López, N. Statistical learning goes beyond the d-band model providing the thermochemistry of adsorbates on transition metals. *Nat. Commun.* **10**, 4687 (2019).
12. Yao, Y. & Goodman, D. W. Direct evidence of hydrogen spillover from Ni to Cu on Ni–Cu bimetallic catalysts. *J. Mol. Catal. Chem.* **383–384**, 239–242 (2014).

13. Hörold, S., Tacke, T. & Vorlop, K. Catalytical removal of nitrate and nitrite from drinking water: 1. Screening for hydrogenation catalysts and influence of reaction conditions on activity and selectivity. *http://dx.doi.org/10.1080/09593339309385367* **14**, 931–939 (1993).
14. Wang, Z., Richards, D. & Singh, N. Recent discoveries in the reaction mechanism of heterogeneous electrocatalytic nitrate reduction. *Catal. Sci. Technol.* **11**, 705–725 (2021).
15. Pintar, A., Batista, J., Levec, J. & Kajiuchi, T. Kinetics of the catalytic liquid-phase hydrogenation of aqueous nitrate solutions. *Appl. Catal. B Environ.* **11**, 81–98 (1996).
16. Martínez, J., Ortiz, A. & Ortiz, I. State-of-the-art and perspectives of the catalytic and electrocatalytic reduction of aqueous nitrates. *Appl. Catal. B Environ.* **207**, 42–59 (2017).
17. Xie, Y., Cao, H., Li, Y., Zhang, Y. & Crittenden, J. C. Highly Selective PdCu/Amorphous Silica−Alumina (ASA) Catalysts for Groundwater Denitration. *Environ. Sci. Technol.* **45**, 4066–4072 (2011).
18. Gauthard, F., Epron, F. & Barbier, J. Palladium and platinum-based catalysts in the catalytic reduction of nitrate in water: Effect of copper, silver, or gold addition. *J. Catal.* **220**, 182–191 (2003).
19. Pintar, A., Batista, J. & Muševič, I. Palladium-copper and palladium-tin catalysts in the liquid phase nitrate hydrogenation in a batch-recycle reactor. *Appl. Catal. B Environ.* **52**, 49–60 (2004).
20. Prüsse, U. & Vorlop, K. D. Supported bimetallic palladium catalysts for water-phase nitrate reduction. *J. Mol. Catal. Chem.* **173**, 313–328 (2001).
21. Sá, J. & Vinek, H. Catalytic hydrogenation of nitrates in water over a bimetallic catalyst. *Appl. Catal. B Environ.* **57**, 247–256 (2005).
22. Cai, F. *et al.* Preparation of PdCu Alloy Nanocatalysts for Nitrate Hydrogenation and Carbon Monoxide Oxidation. *Catal. 2016 Vol 6 Page 96* **6**, 96 (2016).
23. Wang, Z., Evan Ortiz, ab M., Bryan Goldsmith, ab R. & Singh, N. Comparing electrocatalytic and thermocatalytic conversion of nitrate on platinum–ruthenium alloys. *Catal. Sci. Technol.* **11**, 7098–7109 (2021).
24. Ilinich, O. M., Gribov, E. N. & Simonov, P. A. Water denitrification over catalytic membranes: hydrogen spillover and catalytic activity of macroporous membranes loaded with Pd and Cu. *Catal. Today* **82**, 49–56 (2003).

25. Yoshinaga, Y., Akita, T., Mikami, I. & Okuhara, T. Hydrogenation of Nitrate in Water to Nitrogen over Pd–Cu Supported on Active Carbon. *J. Catal.* **207**, 37–45 (2002).
26. Keresszegi, C., Bürgi, T., Mallat, T. & Baiker, A. On the Role of Oxygen in the Liquid-Phase Aerobic Oxidation of Alcohols on Palladium. *J. Catal.* **211**, 244–251 (2002).
27. Mallat, T. & Baiker, A. Catalyst potential measurement: a valuable tool for understanding and controlling liquid phase redox reactions. *Top. Catal.* **8**, 115–124 (1999).
28. An, H., Sun, G., Hülsey, M. J., Sautet, P. & Yan, N. Demonstrating the Electron–Proton-Transfer Mechanism of Aqueous Phase 4-Nitrophenol Hydrogenation Using Unbiased Electrochemical Cells. *ACS Catal.* **12**, 15021–15027 (2022).
29. Ryu, J. *et al.* Thermochemical aerobic oxidation catalysis in water can be analysed as two coupled electrochemical half-reactions. *Nat. Catal. 2021 49* **4**, 742–752 (2021).
30. Adams, J. S., Kromer, M. L., Rodríguez-López, J. & Flaherty, D. W. Unifying Concepts in Electro- and Thermocatalysis toward Hydrogen Peroxide Production. *J. Am. Chem. Soc.* **143**, 7940–7957 (2021).
31. Howland, W. C., Gerken, J. B., Stahl, S. S. & Surendranath, Y. Thermal Hydroquinone Oxidation on Co/N-doped Carbon Proceeds by a Band-Mediated Electrochemical Mechanism. *J. Am. Chem. Soc.* **144**, 11253–11262 (2022).
32. Huang, X. *et al.* Au–Pd separation enhances bimetallic catalysis of alcohol oxidation. *Nature* **603**, 271–275 (2022).
33. Liu, H. *et al.* Electrocatalytic Nitrate Reduction on Oxide-Derived Silver with Tunable Selectivity to Nitrite and Ammonia. *ACS Catal.* **11**, 8431–8442 (2021).
34. Liu, M. J. *et al.* Catalytic Performance and Near-Surface X-ray Characterization of Titanium Hydride Electrodes for the Electrochemical Nitrate Reduction Reaction. *J. Am. Chem. Soc.* **144**, 5739–5744 (2022).
35. Teng, W. *et al.* Selective Nitrate Reduction to Dinitrogen by Electrocatalysis on Nanoscale Iron Encapsulated in Mesoporous Carbon. *Environ. Sci. Technol.* **52**, 230–236 (2018).
36. Li, J. *et al.* Efficient Ammonia Electrosynthesis from Nitrate on Strained Ruthenium Nanoclusters. *J. Am. Chem. Soc.* **142**, 7036–7046 (2020).
37. Butcher, D. P. & Gewirth, A. A. Nitrate reduction pathways on Cu single crystal surfaces: Effect of oxide and Cl−. *Nano Energy* **29**, 457–465 (2016).

38. Vorlop, K.-D. & Prüsse, U. Catalytical removing nitrate from water. in *Environmental Catalysis* vol. Volume 1 195–218 (PUBLISHED BY IMPERIAL COLLEGE PRESS AND DISTRIBUTED BY WORLD SCIENTIFIC PUBLISHING CO., 1999).
39. Pintar, A. & Batista, J. Catalytic stepwise nitrate hydrogenation in batch-recycle fixed-bed reactors. *J. Hazard. Mater.* **149**, 387–398 (2007).
40. Ohyama, J., Kumada, D. & Satsuma, A. Improved hydrogen oxidation reaction under alkaline conditions by ruthenium–iridium alloyed nanoparticles. *J. Mater. Chem. A* **4**, 15980–15985 (2016).
41. Soares, O. S. G. P., Órfão, J. J. M. & Pereira, M. F. R. Activated Carbon Supported Metal Catalysts for Nitrate and Nitrite Reduction in Water. *Catal. Lett.* **126**, 253–260 (2008).
42. Cao, N., Hu, K., Luo, W. & Cheng, G. RuCu nanoparticles supported on graphene: A highly efficient catalyst for hydrolysis of ammonia borane. *J. Alloys Compd.* **590**, 241–246 (2014).
43. Álvarez-Rodríguez, J., Guerrero-Ruiz, A., Rodríguez-Ramos, I. & Arcoya, A. Changes in the selective hydrogenation of citral induced by copper addition to Ru/KL catalysts. *Microporous Mesoporous Mater.* **110**, 186–196 (2008).
44. Zhao, F., Xin, J., Yuan, M., Wang, L. & Wang, X. A critical review of existing mechanisms and strategies to enhance N2 selectivity in groundwater nitrate reduction. *Water Res.* **209**, 117889 (2022).
45. Tokazhanov, G., Ramazanova, E., Hamid, S., Bae, S. & Lee, W. Advances in the catalytic reduction of nitrate by metallic catalysts for high efficiency and N2 selectivity: A review. *Chem. Eng. J.* **384**, 123252 (2020).
46. Ras, E.-J. & Rothenberg, G. Heterogeneous catalyst discovery using 21st century tools: a tutorial. *RSC Adv.* **4**, 5963 (2014).
47. Fan, J. *et al.* Recent Progress on Rational Design of Bimetallic Pd Based Catalysts and Their Advanced Catalysis. *ACS Catal.* **10**, 13560–13583 (2020).
48. Li, Z., Wang, S., Chin, W. S., Achenie, L. E. & Xin, H. High-throughput screening of bimetallic catalysts enabled by machine learning. *J. Mater. Chem. A* **5**, 24131–24138 (2017).
49. Sun, Y., Wei, J., Zhang, J. P. & Yang, G. Optimization using response surface methodology and kinetic study of Fischer–Tropsch synthesis using SiO2 supported bimetallic Co–Ni catalyst. *J. Nat. Gas Sci. Eng.* **28**, 173–183 (2016).

50. Udumula, V. *et al.* Dual Optimization Approach to Bimetallic Nanoparticle Catalysis: Impact of M1/M2 Ratio and Supporting Polymer Structure on Reactivity. *ACS Catal.* **5**, 3457–3462 (2015).